Eur. Phys. J. E **10**, 331–336 (2003)
DOI 10.1140/epje/i2002-10117-x

THE EUROPEAN PHYSICAL JOURNAL E

Structural characterization of a new lipid/DNA complex showing a selective transfection efficiency in ovarian cancer cells

G. Caracciolo[1], D. Pozzi[2], R. Caminiti[3], and A. Congiu Castellano[1,a]

[1] Dipartimento di Fisica and INFM, Università "La Sapienza", P.le A. Moro 5, 00185 Roma, Italy
[2] Dipartimento di Fisica and INFM, Università "Roma Tre", Via della Vasca Navale 84, 00146 Roma, Italy
[3] Dipartimento di Chimica and INFM, Università "La Sapienza", P.le A. Moro 5, 00185 Roma, Italy

Received 28 October 2002 /
Published online: 15 April 2003 –

Abstract. We investigated, for the first time, by using Energy Dispersive X-ray Diffraction, the structure of a new ternary cationic liposome formulated with dioleoyl trimethylammonium propane (DOTAP), 1,2-dioleoyl-3-phosphatidylethanolamine (DOPE) and cholesterol (Chol) (DDC) which has been recently found to have a selective high gene transfer ability in ovarian cancer cells. Our structural results provide a further experimental support to the widely accepted statement that there is not a simple and direct correlation between structure and transfection efficiency and that the factors controlling cationic lipid/DNA (CL-DNA) complexes-mediated gene transfer depend not only on the formulations of the cationic liposomes and their thermodynamic phase, but also significantly on the cell properties.

PACS. 87.14.Cc Lipids – 61.10.-i X-ray diffraction and scattering

1 Introduction

Human gene therapy is defined as the transfer of nucleic acids to somatic cells of a patient providing a therapeutic effect. Nevertheless, this definition is only a part of the complex, a multiphase process which includes the knowledge of the properties of the tissue targeting, cellular trafficking, safety of the vector and other problems. By considering the problem of the vector, it is important to underline that there will not be a "universal vector" but each disease may require a specific modified viral vector or engineering of non-viral carriers. In the future, the perfect gene delivery vector may be a synthetic vector incorporating the advantages acquired by the viruses over millions of years of evolution, but without the pathogenity and the immune reactions produced by the viruses [1].

Among the non-viral carriers, cationic liposomes attract a significant interest because of their unique properties and their efficiency in acting as vehicles for DNA delivery into eukariotic cells [2–7]. High-resolution structural studies indicated the formation of DNA-lipid complexes whose lamellar [8] or columnar inverted hexagonal structures [9] depend upon the lipid composition and the neutral-to-total lipid ratio [10]. Despite the complexity of these researches, it was firstly proposed [8] that the unpredictability of transfection efficiency could be attributed to a lack of knowledge regarding the correlation between the resulting structures of CL-DNA complexes and their mechanism of action and that the quantitative control over the structural nature of the DNA packing could lead to find a direct relation between the structure and the transfection efficiency.

More recently [11], a combined X-ray diffraction and fluorescence optical-microscopy study confirmed distinct interactions between lamellar and inverted columnar hexagonal complexes and mouse fibroblast L-cells, suggesting the existence of a direct correlation between structure and transfection efficiency.

The aim of this work is to provide insights in order to verify if the hypothesis of direct relation between the structure and the transfection efficiency of a DNA-lipid complex has an experimental support. In the absence of this direct correlation, it would be necessary to increase the knowledge of the interactions of the complex with cellular lipids, the mechanism of DNA transfer across plasma and nuclear membranes and the physicochemical properties of the specific target cells in order to design a highly specific gene vector.

We investigated, by using Energy Dispersive X-ray Diffraction (EDXD), the self-assembled structure of a new cationic liposome formulated with dioleoyltrimethylammonium propane (DOTAP), 1,2-dioleoyl-3-phosphatidylethanolamine (DOPE) and cholesterol (Chol) (DOTAP-DOPE-Cholesterol, named DDC). Recently, this new formulation has been found to have a selective

[a] e-mail: a.congiu@caspur.it

high gene transfer ability in ovarian cancer cells [12] with respect to DC-Chol/DOPE liposomes (DC-Chol is a synthetic cationic derivative of cholesterol) which usually provide an efficient vehicle in many gene delivery applications and for this reason are extensively used as controls in varied cell lines [13–15]. Cholesterol-containing cationic liposomes were found to be structurally more stable and effective in dimethyldioctadecylammonium bromide liposomes [16] than those containing DOPE which is a fusogenic lipid that has been shown to destabilize the cellular membranes and enhance transgene expression when added to other cationic lipids *in vitro* [17–19].

2 Experimental

2.1 Cationic-liposomes preparation

The DDC liposomes were prepared with DOTAP (MW = 698.55), DOPE (MW = 744.04) and Chol (MW = 386.7).

Briefly, DOTAP, DOPE and Chol were mixed at a molar ratio 1:0.7:0.3 in chloroform and the obtained organic phase was evaporated at 50 °C in a rotary evaporator. The thin dried film was placed under vacuum to ensure that all traces of solvent had been removed. After hydration with distilled water the solution was sonicated for 10 min.

We also sonicated a deionized-water solution of 5 mg/ml calf-thymus Na-DNA (MW(bp) = 649) for one minute inducing a DNA fragmentation whose length distribution, detected by agarose gel electrophoresis, is between 500–2000 bp. Both lipids and DNA were purchased from Avanti Polar Lipids (Alabaster, AL, USA).

Since DNA carries two negative charges/bp whereas each DOTAP molecule has one positive charge head group, the complex is stoichiometrically neutral only when the numbers of DNA bases and DOTAP molecules are equal or when $\rho = \rho^{\mathrm{iso}} = 2 \times \mathrm{MW(DOTAP)/MW(bp)} = 2.2$.

By mixing adequate amounts of the DNA solution with the cationic liposomes, self-assembled complexes at different ρ values were obtained. We have chosen suitable weight ratios ($\rho = 1.1$, 1.8, 2.2, 3.1, 5.2) in order to extend all our conclusions to the same wide range of ρ investigated by Kim *et al.* [12]. Every sample was then deposited onto the oriented surface (110) of silicon wafers, with a thickness of 150 μm and a diameter $d = 50.8 \pm 0.3$ mm, promoting the formation of ordered structures by drying the samples in a closed chamber under gentle nitrogen flux. Dried samples were partly hydrated as elsewhere proposed (see [20] and references therein).

The followed sample preparation allowed us to obtain high-resolution diffraction patterns. Partly dehydrated samples are commonly used in diffraction experiments (see [21] and references therein) to obtain satisfactory structural pieces of information which are acceptable estimates of the same systems when fully hydrated.

Furthermore, the most prominent and well-estabilished effects of a not full sample hydration are a sensible enhance of the Bragg peak intensities (more diffraction peaks are observed) and a slight decrease in the observed d-spacings [20,21].

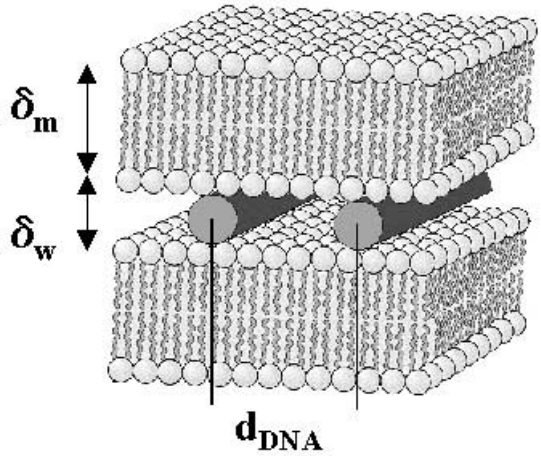

Fig. 1. Schematic of a self-assembled multilayer structure with DNA double strands sandwiched between the charged-lipid bilayers (L_α^c phase): δ_{m} is the thickness of lipid bilayer, δ_{w} is the thickness of the DNA monolayer and d_{DNA} is the inter-helical spacing between two consecutive DNA strands.

2.2 Method

X-ray diffraction experiments were carried out in our laboratory by using an EDXD apparatus [22]. An incident polychromatic X-ray radiation is used and the diffracted beam is energy resolved by a solid-state detector located at a suitable scattering angle. The diffractometer operates in vertical θ/θ geometry and is equipped with an X-ray generator (W-target), a collimating system, step motors, and a solid-state detector connected via an electronic chain to a multichannel analyzer. The X-ray source is a standard Seifert tube operating at 50 kV and 40 mA, whose Bremsstrahlung radiation is used, whereas the detecting system is composed of an EG& G liquid-nitrogen–cooled ultrapure Ge solid-state detector connected to a PC through ADCAM hardware. Both the X-ray tube and the detector can rotate around their common center where a cell is placed. After a preliminary set of measurements, one scattering angle, $\theta = 0.45°$, was selected to investigate the interesting range of the reciprocal space.

The uncertainty associated to θ is $\Delta\theta = 0.001°$ and directly affects the uncertainty Δq associated to the transfer momentum q ($q = \mathrm{const} \times E \times \sin\theta$; const = $1.01354\,\text{Å}^{-1} \times \mathrm{keV}^{-1}$).

Each EDXD scan was collected for $t = 500$ s; during such period no structural modification or damage of the biological samples occur [23].

3 Results

We started by characterizing the structure of the DDC liposomes without DNA.

The EDXD pattern shows two sharp peaks at $q = 0.206\,\text{Å}^{-1}$ and $0.412\,\text{Å}^{-1}$, which correspond to the 001 and 002 Bragg reflections of a highly ordered multilayer structure (Fig. 1) with a membrane stack of periodicity

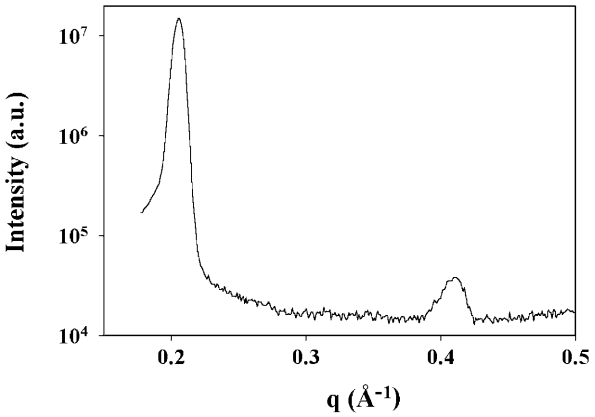

Fig. 2. EDXD pattern of the DDC liposome without DNA: 001 and 002 Bragg reflections of the highly ordered multilamellar structure is shown.

$\mathbf{d} = \delta_{\mathrm{m}} = 30.5\,\text{Å}$ (Fig. 2). The value of $\mathbf{d}$ is smaller than that expectable and this effect is simply interpretable in terms of the preparation of the samples which strongly stabilizes the structure of the liposomes forcing it to loose part of its hydration water; the full hydration of the sample allows to obtain the correct value.

Then we investigated the behaviour of the DDC-DNA complexes in the limit of zero salt concentration as a function of ρ. The EDXD scans at $\rho = 1.1$ and $\rho = 1.8$ (Fig. 3) show the principal peak at $q = 0.131\,\text{Å}^{-1}$ corresponding to the above-mentioned multilamellar structure whose repeat spacing increases to the the value $\mathbf{d} = \delta_{\mathrm{m}} + \delta_{\mathrm{w}} \cong 48\,\text{Å}$, just enough to accommodate the B-DNA molecules between two consecutive lipid bilayers.

Indeed, the uncertainty which affects the repeat distance is directly calculated by combining the instrumental relation $\Delta q = q[\Delta E/E + \mathrm{cotg}\theta\Delta\theta]$ and the Bragg equation; in the present case, the experimental value becomes $\mathbf{d} = (48 \pm 2)\,\text{Å}$.

Our diffraction patterns reflect the DNA condensation between apposed lipid bilayers: the cationic lipid group heads neutralize the phosphate groups on the DNA backbone and the DDC liposomes spontaneously condense DNA into a self-assembled multilayer structure with DNA double strands sandwiched between the charged-lipid bilayers (L_α^{c} phase, Fig. 1). Since the lamellar repeat distance $\mathbf{d}$ is not dependent on the weight ratio ρ, DNA remains tightly bound to lipid bilayers. Furthermore, the diffraction peak due to the membrane stack of the pure lipid is not observed in Figure 3, clearly suggesting that all the lipid is incorporated into the complex which coexists with excess free DNA.

The additional weaker peak, which moves to lower q increasing ρ, arises from the diffraction of a periodic one-dimensional lattice of DNA chains coated between the lipid bilayers and reflects the correlation DNA distance $d_{\mathrm{DNA}} = 2\pi/q_{\mathrm{DNA}}$. In fact, for $\rho < \rho^{\mathrm{iso}}$ the inter-helical distance in the complex decreases, in the presence of excess DNA, with respect to the isoelectric point. Since the free energy of a DNA strand in the complex is lower than in solution, additional DNA molecules enter the complex

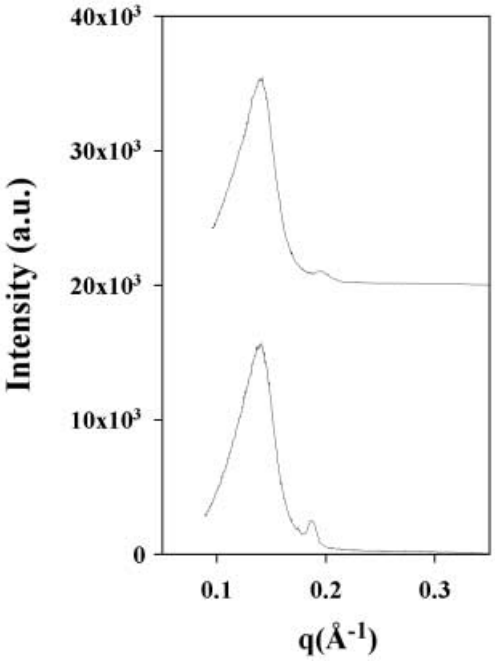

Fig. 3. EDXD scans at $\rho = 1.1$ and $\rho = 1.8$ (from top to bottom): a principal peak corresponding to the multilamellar structure and a weaker peak arising from the diffraction of a periodic one-dimensional lattice of DNA chains coated between the lipid bilayers are shown. In this region of ρ the complex is negatively charged and coexists with excess free DNA.

inducing it to adjust d_{DNA} as long as this overcrowding of DNA strands is balanced by inter-DNA repulsions and the equilibrium value $(d_{\mathrm{DNA}})^-$ is reached. Indeed, the observed DNA distance $d_{\mathrm{DNA}} = 35.1\,\text{Å}$ for $\rho = 1.8$ decreases to $(d_{\mathrm{DNA}})^- = 33.1\,\text{Å}$ for $\rho = 1.1$.

At the isoelectric point the average charge densities of membrane and DNA are exactly matched and the DNA correlation peak is observed at $q = 0.152\,\text{Å}^{-1}$, which corresponds to $(d_{\mathrm{DNA}})^{\mathrm{iso}} = 41.3\,\text{Å}$.

Likewise for $\rho > \rho^{\mathrm{iso}}$ (Fig. 4) the complexes continue absorbing excess lipid as long as lipids enjoy lower free energy into the complex with respect to that in the free bilayer. When the inter-bilayer electrostatic repulsions do not allow further accommodation of the bilayer in the complex, the DNA-DNA spacing reaches the equilibrium distance $(d_{\mathrm{DNA}})^+$ and the system starts to become biphasic.

This is unambigously demonstrated by the scans in Figure 4 corresponding to the values $\rho = 3.1$, 5.2, where we found the expected mobile DNA peak at the same value $q = 0.125\,\text{Å}^{-1}$. It implies that for $\rho = 3.1$ $(d_{\mathrm{DNA}})^+ = 50.2\,\text{Å}$ is reached and the inter-axial distance between DNA strands does not vary any more.

Furthermore, a further peak due to the presence of pure lipid is observed showing that, at some $2.2 < \rho < 3.1$, excess DDC liposomes demix from the membranes instead of remaining within the DDC-DNA complex and separating the DNA strands. In both distinct packing regimes, d_{DNA} varies significantly from $(d_{\mathrm{DNA}})^{\mathrm{iso}}$ (see Fig. 5) and

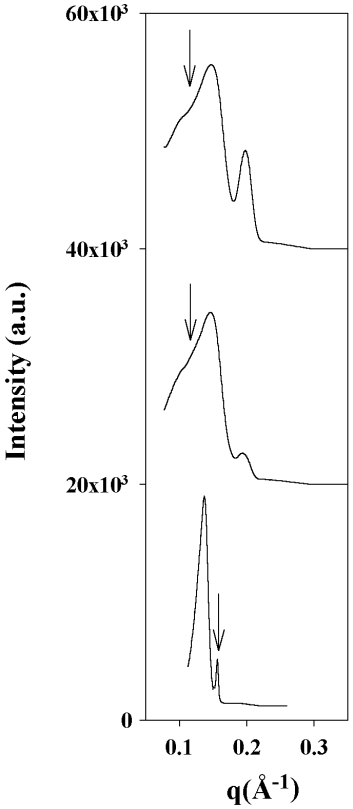

Fig. 4. EDXD scans at $\rho^{\rm iso} = 2.2$, $\rho = 3.1$ and $\rho = 5.2$ (from bottom to top): for $\rho > \rho^{\rm iso}$, the expected mobile DNA peak (indicated by the arrow) and a further peak due to the presence of pure lipid are observed.

the overcharging of the complex leads to a new equilibrium condition starting from which the system is no more compressible.

4 Discussion and conclusions

The CL-DNA complexes have been exstensively studied from a theoretical point of view [24–29] leading to a detailed explanation of the structure and phase evolution in aqueous solutions. Anyway, a simple thermodynamic model which captures the above-explained basic physics principles governing the multilamellar cationic liposomes-DNA complexes has been elsewhere described [28] and succesfully applied [30,31]. This model, altough approximate, does contain the essential features of the complex-DNA and complex-bilayer coexistence allowing to obtain closed expressions for the equilibrium distances $(d_{\rm DNA})^+$ and $(d_{\rm DNA})^-$:

$$(d_{\rm DNA})^+ = (d_{\rm DNA})^{\rm iso} \Big/ \big(1 - \exp\big(-(1 + (\pi a/2l_{\rm B})/(2\delta_{\rm w} m_+))\big)\big)\,, \quad (1)$$

$$(d_{\rm DNA})^- = (d_{\rm DNA})^{\rm iso} \times \big(1 - \exp\big(-(1 + (\pi a/2l_{\rm B})m_+/2\delta_{\rm w} m_-^2)\big)\big)\,, \quad (2)$$

where $a \sim 70\,\text{Å}^2$ is the area of the lipid positive charge/head group, $l_{\rm B}$ is the Bjerrum length, $\delta_{\rm w}$ is the distance between apposed lipid surfaces (see Fig. 1), m_+ is the charged-lipid mole fraction and m_- is the dimensionless charge density of the DNA surface.

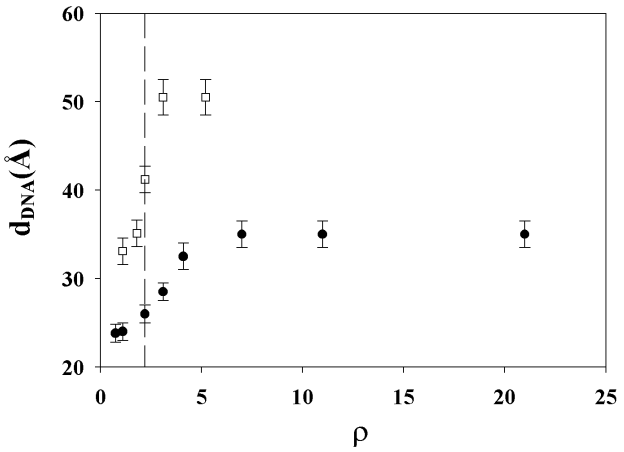

Fig. 5. Variation of DNA packing with ρ: squares, $d_{\rm DNA}$ as a function of ρ for DDC-DNA complexes; circles, $d_{\rm DNA}$ as a function of ρ for DOTAP-DNA complexes [31]. Both the complexes are one-phase in the region of the isoelectric point coexisting with lipid at higher ρ and with DNA at lower ρ. The vertical dashed line indicates the isoelectric point.

From the previous equations it follows that $((d_{\rm DNA})^+/(d_{\rm DNA})^{\rm iso}) \sim 1.20$ in the region $\rho > \rho^{\rm iso}$. Experimental values of $(d_{\rm DNA})^+ = 50.2\,\text{Å}$ and $(d_{\rm DNA})^{\rm iso} = 41.3\,\text{Å}$ determine $((d_{\rm DNA})^+/(d_{\rm DNA})^{\rm iso})_{\rm exp} \sim 1.21$, which is in good agreement with the predicted value.

The experimental value of $(d_{\rm DNA})^{\rm iso}$ is in very good agreement with the theoretical value calculated strarting from the expression derived by Koltover and coworkers [30]:

$$(d_{\rm DNA})^{\rm iso} = (A_{\rm D}\rho_{\rm D}/\rho_{\rm L}\delta_{\rm m}) \times \rho^{\rm iso}/(1 - \Phi)\,, \quad (3)$$

where $A_{\rm D}$ is the cross-section area of the DNA molecule, $\rho_{\rm D}$ and $\rho_{\rm L}$ are the densities of the DNA and the lipid, $\delta_{\rm m}$ is the above-calculated thickness of the lipid bilayer and Φ = (neutral lipid/ total lipid) (w/w).

Using equation (3) we obtain $(d_{\rm DNA})^{\rm iso} = 40.1\,\text{Å}$ which is in good agreement with our experimental finding.

In the region $\rho < \rho^{\rm iso}$, the measured equilibrium distance is $((d_{\rm DNA})^-/(d_{\rm DNA})^{\rm iso})_{\rm exp} \sim 0.74$ which is consistent with the predicted value $((d_{\rm DNA})^-/(d_{\rm DNA})^{\rm iso}) \sim 0.73$. Comparing the variation of $d_{\rm DNA}(\rho)$ reported in Figure 5 with that previously obtained by Koltover [30] for the DOTAP-DOPC complex at a weight fraction of the neutral lipid $\Phi_{\rm PC}$ = (weight of DOPC/total lipid weight) = 0.5, which is approximatively the same of our case ($\Phi = 0.52$), no significant difference between the two patterns appears. It is a strong evidence that, in the case of lipoplexes, the degree of overcharging is only dependent on the membrane charge density regulated by the ratio of neutral-to-total lipid in the bilayers. Figure 5 also shows that the slope of the $d_{\rm DNA}(\rho)$ increase is directly proportional to the percentage of neutral lipid in the complex up to the minimal value observed for the pure DOTAP-DNA

complexes [31], where no neutral lipid is added. Moreover, it ensures that the obtained $(d_{\mathrm{DNA}})^{-}$ is just the equilibrium distance between the DNA rods.

In conclusion, over the range of ρ investigated, all the complexes were arranged in a L_{α}^{c} multilamellar phase with only different DNA packing regimes: our experimental findings show that the electrostatic repulsions set a strict constraint on the excess lipid or DNA that the neutral DDC-DNA complex can accommodate resulting as the driving forces for this spontaneous self-assembly.

DDC liposomes appeared to be a promising non-viral vector for treating ovarian adenocarcinoma and, despite our structural results, it was evidenced that their transfection efficiency changes as a function of the total lipid/DNA weight ratio [12]. Indeed, when the complexes are charge neutral they tend to aggregate into large assemblies implying a reduced expression. On increasing the weight ratio, a higher expression of the transgene was observed because of the inter-liposomes repulsions which force them to remain individual or just linked by few [32]. The optimal transfection of DNA was achieved next to the isoelectric point. Anyway, at a ratio of DDC to DNA over 6:1 (which refers to our value of $\rho \sim 3.1$), citotoxicity of DDC in ovarian cancer cells was found. This reduction of expression reflects lipid toxicity and this result is in line with the evidenced coexistence of the complex with bare lipid (see Fig. 4).

Since the here adopted sample preparation does not severely affect the structure of the CL-DNA complexes, as above explained, it ensures that our structural findings are a reasonable estimation of the lipoplexes employed in gene delivery applications. Therefore, by considering our structural characterization, it could be deduced that a simple correlation between structure and transfection efficiency does not exist. In fact, DDC liposomes with a multilayer structure exhibited an over fourfold increase in expressions levels in OVCAR-3 and SK-OV-3 cells, compared with DC-Chol/DOPE liposomes (3:2 molar ratio), which are known to self-assemble into a columnar inverted hexagonal phase ($H_{\mathrm{II}}^{\mathrm{C}}$) (our unpublished results confirm this arrangement).

On the other hand, it has been shown [33] that DC-Chol/DOPE complexes transfect human tracheal epithelial cells more efficiently than other cationic lipid-DNA complexes which are well characterized by a multilamellar L_{α}^{c} phase.

Moreover, DDC liposomes showed a lower transfection efficiency in other cell lines (NIH3T3, NCI-NIH:522 and HepG2) suggesting that a transfecting vehicle composed of DOTAP, DOPE and Chol is an efficient vector system in ovarian cancer cells rather than in other cell types.

Our results combined with the above-mentioned ones indicate that there is not a simple and direct correlation between structure and transfection efficiency and that the factors controlling cationic liposome/DNA complex-mediated gene transfer depend not only on the formulations of the cationic liposome and their thermodynamic phase, but must also depend significantly on their interaction with the cell and therefore on the cell properties.

Recently, it has been reported that also the target cells cycle status can play a role on the transfection efficiency [34].

In conclusion, our results confirm that the research concerning the gene therapy must be focused on the knowledge not only of the DNA-vector (viral or non-viral) properties, in particular of its structure, but also of the biological properties of the target cells and therefore of the cell-vector interaction.

References

1. G.M. Rubanyi, Mol. Asp. Med. **22**, 113 (2001).
2. P.L. Felgner, T.R. Gadek, M. Holm, R. Roman, H.W. Chan, M. Wenz, J.P. Northrop, G.M. Ringold, M. Danielsen, Proc. Natl. Acad. Sci. USA **84**, 7413 (1987).
3. P.L. Felgner, Hum. Gene Ther. **7**, 1791 (1996).
4. P.L. Felgner, G.M. Ringold, Nature **331**, 461 (1989).
5. X. Gao, L. Huang, Biochem. Biophys. Res. Commun. **179**, 280 (1991).
6. F.D. Ledley, Hum. Gene Ther. **6**, 1129 (1995).
7. D.D. Lasic, H. Strey, M.C. Stuart, R. Podgornik, P.M. Frederik, J. Am. Chem. Soc. **119**, 832 (1997).
8. J.O. Radler, I. Koltover, T. Salditt, C.R. Safinya, Science **275**, 810 (1997).
9. I. Koltover, T. Salditt, J.O. Radler, C.R. Safinya, Science **281**, 78 (1998).
10. C.R. Safinya, Curr. Opin. Struct. Biol. **11**, 440 (2001).
11. A.J. Lin., N.L. Slack, A. Ahmad, I. Koltover, C.X. George, C.E. Samuel, C.R. Safinya, J. Drug Target **8**, 13 (2000).
12. C.K. Kim, Kh. H. Hider, S.H. Choi, E.J. Choi, W.S. Ahn, Y.B. Kim, Gynec. Onc. **84**, 85 (2002).
13. P.S. Ajmaniaa, J.A. Hughes, Neurochem. Res. **24**, 699 (1999).
14. K.D. Murray, A. Mc Quillin, L. Stewart, C.J. Etheridge, R.G. Cooper, A.D. Miller, H.M. Gurling, Gene Ther. **6**, 190 (1999).
15. J.S. Choi, E.J. Lee, H.S. Jang, J.S. Park, Bioconjug. Chem. **12**, 108 (2001).
16. K. Hong, W. Zheng, A. Baker, W. Papahadjopoulos, FEBS Lett. **400**, 233 (1997).
17. S.W. Hui, M. Langner, Y.L. Zhao, E. Hurley, K. Chan, Biophys. J. **71**, 590 (1996).
18. K.W.C. Mok, P.R. Cullis, Biophys. J. **73**, 2534 (1997).
19. S. Simões, V. Slepushkin, R. Gaspar, M.C. Pedroso de Lima, N. Düzgünes, Gene Ther. **5**, 955 (1998).
20. J. Katsaras, Biophys. J. **75**, 2157 (1998).
21. G. Pabst, M. Rappolt, H. Amenitsch, P. Laggner, Phys. Rev. E **62**, 4000 (2000).
22. R. Caminiti, V. Rossi Alberini, Int. Rev. Phys. Chem. **18**, 263 (1999).
23. G. Caracciolo, G. Amiconi, L. Bencivenni, G. Boumis, R. Caminiti, E. Finocchiaro, B. Maras, C. Paolinelli, A. Congiu Castellano, Eur. Biophys. J. **30**, 163 (2001).
24. N. Dan, Biophys. J. **71**, 1267 (1996).
25. N. Dan, Biophys. J. **73**, 1842 (1997).
26. N. Dan, Biochim. Biophys. Acta **1369**, 34 (1998).
27. R. Bruinsma, Eur. Phys. J. B **4**, 75 (1998).
28. D. Harries, S. May, W.M. Gelbart, A. Ben-Shaul, Biophys. J. **75**, 159 (1998).
29. S. May, D. Harries, A. Ben-Shaul, Biophys. J. **78**, 1681 (2000).

30. I. Koltover, T. Salditt, C.R. Safinya, Biophys. J. **77**, 915 (1999).
31. G. Caracciolo, R. Caminiti, D. Pozzi, M. Friello, F. Boffi, A. Congiu Castellano, Chem. Phys. Lett. **351**, 222 (2002).
32. C.R. Safinya, I. Koltover, J.O. Radler, Curr. Opin. Colloid Interface Sci. **3**, 69 (1998).
33. A. Colosimo, A. Serafino, F. Sangiuolo, S. Di Sario, E. Bruscia, P. Amicucci, G. Novelli, B. Dallapiccola, G. Mossa, Biochim. Biophys. Acta **1419**, 186 (1999).
34. I. Mortimer, P. Tam, I. MacLachlan, R.W. Graham, E.G. Saravolac, P.B. Joshi, Gene Ther. **6**, 403 (1999).